SCIENCE CHINA
Physics, Mechanics & Astronomy

• Article •

November 2023 Vol. 66 No. 11: 112011
https://doi.org/10.1007/s11433-023-2220-y

Vector meson effects on multi-Skyrmion states from the rational map ansatz

Jun-Shuai Wang[1,2], and Yong-Liang Ma[2,3*]

[1] *College of Physics, Jilin University, Changchun 130012, China;*
[2] *School of Fundamental Physics and Mathematical Sciences, Hangzhou Institute for Advanced Study, University of Chinese Academy of Sciences (UCAS), Hangzhou 310024, China;*
[3] *TaiJi Laboratory for Gravitational Wave Universe (Beijing/Hangzhou), UCAS, Beijing 100049, China*

Received June 17, 2023; accepted September 11, 2023; published online September 15, 2023

The roles of the lightest vector mesons ρ and ω in the multi-Skyrmion states are studied using the hidden local symmetry approach up to the next-to-leading order, including the homogeneous Wess-Zumino terms. The low-energy constants in the effective field theory are determined using the Sakai-Sugimoto model and the flat-space five-dimensional Yang-Mills action. With only two inputs, m_ρ and f_π, it is possible to determine all low-energy constants without ambiguity. The vector meson effects can be investigated by sequentially integrating vector mesons, and their geometry can be elucidated by comparing the results using the low-energy constants estimated from the Sakai-Sugimoto model and the flat-space five-dimensional Yang-Mills action. We found that the ρ meson reduces the masses of the multi-Skyrmion states and increases the overlaps of their constituents, whereas the ω meson repulses the constituents of the multi-Skyrmion states and increases their masses. Therefore, these vector mesons are crucial in the Skyrme model approach to nuclei. We also found that the warping factor, an essential element in the holographic model of QCD, affects the properties of the multi-Skyrmion states and cannot be ignored.

vector meson, multi-Skyrmion state, rational map, hidden local symmetry

PACS number(s): 12.39.Dc, 12.39.Fe, 21.45.-v, 21.60.-n

Citation: J.-S. Wang, and Y.-L. Ma, Vector meson effects on multi-Skyrmion states from the rational map ansatz, Sci. China-Phys. Mech. Astron. **66**, 112011 (2023), https://doi.org/10.1007/s11433-023-2220-y

1 Introduction

The Skyrme model [1, 2] as a nonlinear theory of mesons based on the chiral symmetry breaking of QCD provides a unified framework to study the single baryons, multi-baryon states and nuclear matter [3-7] when the skyrmions are regarded as baryons in the limit of large number of colors N_c [8-10].

In the Skyrmion approach to nuclear physics, it is found that the vector mesons play indispensable roles [11-17]. The vector meson effects can be studied without ambiguity using effective models in higher dimensions. Researchers [18-20] showed the Skyrmion properties by dimensionally deconstructing a five-dimensional holographic model, the Sakai-Sugimoto model [21, 22], into a four-dimensional effective theory of vector mesons, the hidden local symmetry (HLS) approach [23-25]. In this approach, all the low-energy constants (LECs) can be fixed with only two inputs f_π and m_ρ except the parameter a, which proves that any physical quantities calculated with the HLS Lagrangian induced from hQCD models are independent of it [20]. The inclusion of the ρ

*Corresponding author (email: ylma@ucas.ac.cn)

meson reduces the soliton mass, which brings the Skyrmion closer to the Bogomol'nyi-Prasad-Sommerfield soliton; however, the ω meson increases the soliton mass. Similarly, using a $(4+1)$-dimensional Yang-Mills theory, which may be written as a $(3+1)$-dimensional BPS Skyrme model, it is found that the iso-vector hadron resonances ρ and a_1 suppress the Skyrmion mass and the more resonances included further suppression [26, 27].

The Skyrmion approach to the multi-Skyrmion states is achieved using the product ansatz [1, 28, 29] or the rational map ansatz [30-32] since the multi-Skyrmion states obtained by extending the boundary conditions of hedgehog ansatz are unstable [33]. A generic property of the multi-Skyrmion states is that their shapes are not spherical like the $B = 1$ Skyrmion but have special symmetries. Moreover, it is found that the states with large baryon numbers have a hollow structure in the chiral limit, and this hollow structure may be unstable when the physical pion mass is considered (see, e.g., ref. [34] for a review). Moreover, this hollow structure is significant for understanding the possible multilayer structure of neutron stars [35] considering that Skyrmion matter at high density has a sheet structure composed of half-skyrmions [36].

Regarding the standard Skyrme model, the multi-Skyrmion states were investigated using the rational map ansatz [30]. Although some states are not bound, another approach using different numerical algorithms did not find these unbounded states [37]. When the Skyrme model is extended to include the positive pion mass, the structure of the multi-Skyrmion states is changed [38] and the α-cluster structure of nuclei is found [34]. Moreover, when the Skyrme model is extended to include the vector meson ρ using an effective $(3+1)$-dimensional BPS theory truncated from a $(4+1)$-dimensional Yang-Mills theory, it is found that the masses of the multi-Skyrmion states with baryon number upto $B = 4$ are suppressed [27, 39]. In the same framework that includes massive pions, the clustering structure of the light nuclei can be obtained, and the binding energies are very close to the nuclear data [40].

Although many accesses to the multi-Skyrmion states have been conducted in the literature, there are still some ambiguities, which are as follows: What is the effect of the iso-scalar vector meson ω, which is responsible for repulsive force in nuclear physics on the multi-baryon states with baryon number $B > 2$? Are the characters of the multi-Skyrmion states changed when the ρ is considered an independent degree of freedom or integrated out from the theory such that its effect is hidden in the Skyrme parameter? What is the influence of the geometry in the five-dimension that affects the values of the LECs? In this research, we have systematically clarified these ambiguities using the rational map ansatz and leave the discussion of the structures of the multi-Skyrmion states at global minima to future work.

We used the HLS approach for the vector mesons in $(3+1)$-dimension developed in the nonlinear realization of chiral symmetry [23-25]. The Lagrangian is considered up to the next-to-leading order, including the homogeneous Wess-Zumino (hWZ) terms responsible for the omega meson effect. To control the ambiguities for the LECs, we resort to the effective models in $(4+1)$-dimension, i.e., the Sakai-Sugimoto (SS) model and the $(4+1)$-dimensional Yang-Mills theory (BPS model). We could check the resonance effects by integrating the resonance in order by comparing the results from the HLS with the LECs fixed using a certain effective model. Moreover, the difference between the results obtained using the LECs yielded from the SS and BPS models shows the effect of the warping factor in the five dimensions.

The rest of this paper is arranged as follows. In sect. 2, we outlined the effective field theory used in this work and rational map ansatz up to baryon number $B = 8$. In sect. 3, we listed our numerical results and compared these values obtained from different models. Our conclusion and discussion are given in sect. 4. The expression of the masse of the multi-Skyrmion state is shown in Appendix.

2 The hidden local symmetry approach for vector mesons

To see the effects of the vector mesons rho and omega on the multi-Skyrmion states, among a variety of effective approaches, we used the HLS method to include these vector mesons in the chiral effective theory [23-25]. We considered the HLS up to the next-to-leading order, including the hWZ terms, which are responsible for the contribution from omega meson.

The full symmetry considered in this research is $G_{\rm full} = [SU(2)_L \times SU(2)_R]_{\rm chiral} \times [U(2)_V]_{\rm HLS}$ with $[U(2)_V]_{\rm HLS}$ being the HLS. The HLS Lagrangian with symmetry $G_{\rm full}$ can be written in terms of the Maurer-Cartan 1-forms

$$\begin{aligned}\hat{\alpha}_{\perp\mu} &= \frac{1}{2\mathrm{i}}\left(D_\mu\xi_R\cdot\xi_R^\dagger - D_\mu\xi_L\cdot\xi_L^\dagger\right),\\ \hat{\alpha}_{\parallel\mu} &= \frac{1}{2\mathrm{i}}\left(D_\mu\xi_R\cdot\xi_R^\dagger + D_\mu\xi_L\cdot\xi_L^\dagger\right),\end{aligned} \tag{1}$$

with the chiral fields $\xi_{L,R}$, which in the unitary gauge are written as:

$$\xi_L^\dagger = \xi_R \equiv \xi = \mathrm{e}^{\mathrm{i}\pi/2f_\pi}, \tag{2}$$

where $\pi = \boldsymbol{\pi}\cdot\boldsymbol{\tau}$ with $\boldsymbol{\tau}$ being the Pauli matrices. Without considering the external sources, we obtain the covariant derivative as:

$$D_\mu\xi_{L,R} = \left(\partial_\mu - \mathrm{i}V_\mu\right)\xi_{L,R}, \tag{3}$$

with V_μ being the gauge boson of the HLS. After breaking the HLS and in the unitary gauge, the field V_μ is expressed in terms of the vector meson fields as:

$$V_\mu = \frac{g}{2}\left(\omega_\mu + \rho_\mu\right), \tag{4}$$

with

$$\rho_\mu = \boldsymbol{\rho}_\mu \cdot \boldsymbol{\tau} = \begin{pmatrix} \rho_\mu^0 & \sqrt{2}\rho_\mu^+ \\ \sqrt{2}\rho_\mu^- & -\rho_\mu^0 \end{pmatrix}. \tag{5}$$

In addition to the two Maurer-Cartan 1-forms $\hat{\alpha}_{\perp,\parallel,\mu}$, due to the gauge field of the HLS, the third block in the construction of the HLS Lagrangian is the field strength tensor

$$V_{\mu\nu} = \partial_\mu V_\nu - \partial_\nu V_\mu - \mathrm{i}\left[V_\mu, V_\nu\right]. \tag{6}$$

With the above discussion, the HLS Lagrangian, which will be used in this study up to $O(p^4)$ as in ref. [25], can be constructed

$$\mathcal{L} = \mathcal{L}_{(2)} + \mathcal{L}_{(4)} + \mathcal{L}_{\mathrm{anom}}. \tag{7}$$

The leading order Lagrangian, the $O(p^2)$ terms, $\mathcal{L}_{(2)}$ in the chiral limit, which will be considered in this study

$$\mathcal{L}_{(2)} = f_\pi^2 \mathrm{Tr}(\hat{\alpha}_{\perp\mu}\hat{\alpha}_\perp^\mu) + a f_\pi^2 \mathrm{Tr}(\hat{\alpha}_{\parallel\mu}\hat{\alpha}_\parallel^\mu) - \frac{1}{2g^2}\mathrm{Tr}(V_{\mu\nu}V^{\mu\nu}), \tag{8}$$

where f_π is the pion decay constant, a is the parameter of the HLS, g is the coupling constant of the hidden local gauge field—the vector meson field. For the $O(p^4)$ Lagrangian, we only considered the terms having one trace since the terms including two traces are suppressed by $1/N_c$. Then, the $O(p^4)$ Lagrangian was used as given by

$$\mathcal{L}_{(4)} = \mathcal{L}_{(4)y} + \mathcal{L}_{(4)z}, \tag{9}$$

where

$$\begin{aligned}\mathcal{L}_{(4)y} =& y_1 \mathrm{Tr}\left[\hat{\alpha}_{\perp\mu}\hat{\alpha}_\perp^\mu \hat{\alpha}_{\perp\nu}\hat{\alpha}_\perp^\nu\right] + y_2 \mathrm{Tr}\left[\hat{\alpha}_{\perp\mu}\hat{\alpha}_{\perp\nu}\hat{\alpha}_\perp^\mu \hat{\alpha}_\perp^\nu\right] \\ &+ y_3 \mathrm{Tr}\left[\hat{\alpha}_{\parallel\mu}\hat{\alpha}_\parallel^\mu \hat{\alpha}_{\parallel\nu}\hat{\alpha}_\parallel^\nu\right] + y_4 \mathrm{Tr}\left[\hat{\alpha}_{\parallel\mu}\hat{\alpha}_{\parallel\nu}\hat{\alpha}_\parallel^\mu \hat{\alpha}_\parallel^\nu\right] \\ &+ y_5 \mathrm{Tr}\left[\hat{\alpha}_{\perp\mu}\hat{\alpha}_\perp^\mu \hat{\alpha}_{\parallel\nu}\hat{\alpha}_\parallel^\nu\right] + y_6 \mathrm{Tr}\left[\hat{\alpha}_{\perp\mu}\hat{\alpha}_{\perp\nu}\hat{\alpha}_\parallel^\mu \hat{\alpha}_\parallel^\nu\right] \\ &+ y_7 \mathrm{Tr}\left[\hat{\alpha}_{\perp\mu}\hat{\alpha}_{\perp\nu}\hat{\alpha}_\parallel^\nu \hat{\alpha}_\parallel^\mu\right] \\ &+ y_8 \left\{\mathrm{Tr}\left[\hat{\alpha}_{\perp\mu}\hat{\alpha}_\parallel^\mu \hat{\alpha}_{\perp\nu}\hat{\alpha}_\parallel^\nu\right] + \mathrm{Tr}\left[\hat{\alpha}_{\perp\mu}\hat{\alpha}_{\parallel\nu}\hat{\alpha}_\perp^\nu \hat{\alpha}_\parallel^\mu\right]\right\} \\ &+ y_9 \mathrm{Tr}\left[\hat{\alpha}_{\perp\mu}\hat{\alpha}_{\parallel\nu}\hat{\alpha}_\perp^\mu \hat{\alpha}_\parallel^\nu\right],\end{aligned} \tag{10}$$

$$\mathcal{L}_{(4)z} = \mathrm{i}z_4 \mathrm{Tr}\left[V_{\mu\nu}\hat{\alpha}_\perp^\mu \hat{\alpha}_\perp^\nu\right] + \mathrm{i}z_5 \mathrm{Tr}\left[V_{\mu\nu}\hat{\alpha}_\parallel^\nu \hat{\alpha}_\parallel^\nu\right]. \tag{11}$$

For the anomalous parity part, the Lagrangian $\mathcal{L}_{\mathrm{anom}}$ has expression

$$\mathcal{L}_{\mathrm{anom}} = \frac{N_c}{16\pi^2}\sum_{i=1}^{3} C_i \mathcal{L}_i, \tag{12}$$

where

$$\mathcal{L}_1 = \mathrm{iTr}\left[\hat{\alpha}_L^3\hat{\alpha}_R - \hat{\alpha}_R^3\hat{\alpha}_L\right], \tag{13a}$$

$$\mathcal{L}_2 = \mathrm{iTr}\left[\hat{\alpha}_L\hat{\alpha}_R\hat{\alpha}_L\hat{\alpha}_R\right], \tag{13b}$$

$$\mathcal{L}_3 = \mathrm{Tr}\left[F_V(\hat{\alpha}_L\hat{\alpha}_R - \hat{\alpha}_R\hat{\alpha}_L)\right], \tag{13c}$$

with the 1-form and 2-form fields

$$\hat{\alpha}_L = \hat{\alpha}_\parallel - \hat{\alpha}_\perp, \quad \hat{\alpha}_R = \hat{\alpha}_\parallel + \hat{\alpha}_\perp, \quad F_V = dV - \mathrm{i}V^2. \tag{14}$$

To study the properties of the multi-Skyrmion states using the Lagrangian (7) from the rational map ansatz, we parameterized the chiral field as [30]:

$$\xi(r) = \exp\left[\mathrm{i}\boldsymbol{\tau}\cdot\hat{\boldsymbol{n}}\frac{F(r)}{2}\right], \tag{15}$$

where

$$\hat{\boldsymbol{n}} = \frac{1}{1+|R|^2}\left(2\mathrm{Re}(R), 2\mathrm{Im}(R), 1-|R|^2\right), \tag{16}$$

R represents the rational map, a function of the complex coordinate z on a Riemann unit two-sphere, and r is the distance from the origin. For a baryon number B state, the rational map $R(z) = p/q$ has p and q that are polynomial in z such that $\max[\deg(p), \deg(q)] = N$ and p and q have no common factors. Explicitly, for $B = 1, 2, \cdots, 8$, $R(z)$ has the following form [30]:

$N = 1$ $R(z) = z$, the hadgehog map.

$N = 2$ $R(z) = \frac{z^2-a}{-az^2+1}$, with a being a real parameter and $-1 \le a \le 1$.

$N = 3$ $R(z) = \frac{\sqrt{3}az^2-1}{z(z^2-\sqrt{3}a)}$, with a being a complex parameter.

$N = 4$ $R(z) = c\frac{z^4+2\sqrt{3}iz^2+1}{z^4-2\sqrt{3}iz^2+1}$, with c being a real parameter.

$N = 5$ $R(z) = \frac{z(z^4+bz^2+a)}{az^4-bz^2+1}$, with a and b as real parameters.

$N = 6$ $R(z) = \frac{z^4+ia}{z^2(iaz^4+1)}$, with a being a real parameter.

$N = 7$ $R(z) = \frac{bz^6-7z^4-bz^2-1}{z(z^6+bz^4+7z^2-b)}$, with b being a complex parameter.

$N = 8$ $R(z) = \frac{z^6-a}{z^2(az^6+1)}$, with a being a real parameter.

For the vector mesons ρ and ω, we applied the following configurations [41,42]:

$$\omega_\mu = W(r)\delta_{0\mu}, \quad \rho_0 = 0, \quad \rho_i = -\frac{G(r)}{g}\boldsymbol{\tau}\cdot(\hat{\boldsymbol{n}}\times\partial_i\hat{\boldsymbol{n}}). \tag{17}$$

The profiles of the meson fields satisfied the following boundary conditions:

$$F(0) = \pi, \quad F(\infty) = 0,$$

$$G(0) = 2, \quad G(\infty) = 0, \qquad (18)$$
$$W'(0) = 0, \quad W(\infty) = 0.$$

Using the effective Lagrangian (7) and the antsatz (16) and (17), one can easily derive the expression for the mass of the multi-Skyrmion state. The explicit formula is given in Appendix. By minimizing the mass of the multi-Skyrmion state subject to the boundary conditions (19) one can obtain the profiles of $F(r), G(r)$ and $W(r)$ and consequently, the mass of the multi-Skyrmion states once the LECs are given.

3 Numerical results for the multi-Skyrmion states

3.1 The model and low-energy constants

To calculate the properties of the multi-Skyrmion states described in Appendix, we first need to know the values of the LECs. Lagrangian (7) contains 18 parameters, $f_\pi, a, g, y_1, y_2, \cdots, y_9, z_4, z_5, c_1, c_2, c_3$ and the vector meson mass $m_V = m_\rho \simeq m_\omega$. As the vector meson mass satisfies the relation

$$m_V^2 = ag^2 f_\pi^2 \qquad (19)$$

and the empirical values of f_π and $m_V = m_\rho \simeq m_\omega$ are well known; 15 parameters remain, and we have not been able to estimate the values of these parameters thus far.

Therefore, to finalize the numerical calculation, we estimated the LECs from the dual models of QCD in five dimensions, explicitly, the holographic model of QCD from the top-down approach—the Sakai-Sugimoto (SS) model [21]. For comparative purposes, we also estimated the LECs using the Bogomol'nyi-Prasad-Sommerfield (BPS) model [43]—the Yang-Mills theory in five dimensions to show the effect of geometry. We denoted the HLS with parameters determined from the SS model as $\mathrm{HLS_{SS}}$ and that from the BPS model as $\mathrm{HLS_{BPS}}$. Due to the special structure of the 5D Dirac-Born-Infeld part of the SS model and the gauge invariance of the (4+1)-dimensional Yang-Mills theory, the LECs in HLS have the following relations:

$$y_1 = -y_2, \quad y_3 = -y_4,$$
$$y_5 = 2y_8 = -y_9, \quad y_6 = -(y_5 + y_7). \qquad (20)$$

Moreover, the omega meson effect only enters through the hWZ terms. In the five-dimensional models, the parameter a is related to the normalization of the eigenfunction of the vector mode; however, the physical quantities calculated with the HLS induced from the five-dimensional models are independent of the parameter a, although the values of the LECs depend on it [20]. With the choice $a = 2$, which reproduces the Kawarabayashi-Suzuki-Riazzudin-Fayyazudin relation and the rho meson dominance in the pion electromagnetic form factor, we present the values of the LECs estimated from the SS model and the BPS model in Table 1 [20].

To investigate the resonance effects on the multi-Skyrmion states, we considered three versions of HLS in the following.

(1) **HLS(π, ρ, ω)** The HLS with all the π, ρ and ω fields.

(2) **HLS(π, ρ)** The HLS with π and ρ fields, which is obtained by integrating out ω field from, or equivalently dropping the hWZ terms in, the Lagrangian (7).

(3) **HLS(π)** The HLS with only π, which is obtained from HLS(π, ρ, ω) by integerating out both ρ and ω fields [25]. In this scenario, the Skyrmion parameter was affected by the y_1, y_2, and z_4 terms in addition to the kinetic term of the vector mesons [20]. In this case, the Skyrme parameter $e = 7.31$ in $\mathrm{HLS_{SS}}(\pi)$ and $e = 10.02$ in $\mathrm{HLS_{BPS}}(\pi)$.

3.2 Numerical results

With the above-estimated LECs, the multi-Skyrmion states can be calculated. To obtain the profile functions, we used the finite element method [44] to minimize the total static energy of the system described in Appendix concerning the boundary conditions (19). The advantage of the finite element method is that only the first-order ordinary differential equations (ODEs) must be handled. If additional resonances are desired, it is not necessary to derive the tedious equation of motion (second-order ODEs) again.

3.2.1 Effects from the hadron resonances

To investigate the resonance effects, we first considered the properties of the multi-Skyrmion states using the HLS with the LECs determined from the SS model. Table 2 depicts the masses of the multi-Skyrmion states for baryon numbers $B = 1, 2, \cdots, 8$.

Table 1 Low energy constants of the HLS Lagrangian at $O(p^4)$ with $a = 2$

Model	y_1	y_3	y_5	y_6	z_4	z_5	c_1	c_2	c_3
SS model	−0.001096	−0.002830	−0.015917	+0.013712	0.010795	−0.007325	+0.381653	−0.129602	0.767374
BPS model	−0.071910	−0.153511	−0.012286	−0.196545	0.090338	−0.130778	−0.206992	+3.031734	1.470210

Table 2 Masses of the multi-Skyrmion states in $\mathrm{HLS_{SS}}$ (in unit of $4\pi f_\pi^2/m_\rho$). Only the hadron degrees of freedom are explicitly written for simplicity

Model	B							
	1	2	3	4	5	6	7	8
(π,ρ,ω)	8.59	16.90	24.94	32.44	40.58	48.37	55.56	63.71
(π,ρ)	6.04	12.37	18.44	23.65	30.04	35.83	40.64	47.07
(π)	6.67	13.08	19.23	24.59	31.03	36.92	41.93	48.39

Comparing the results from $\mathrm{HLS_{SS}}(\pi)$ and $\mathrm{HLS_{SS}}(\pi,\rho)$ shows that the attractive force from the rho meson decreases the masses of the multi-Skyrmion states. This is consistent with the knowledge gained from understanding the nuclear force and calculating the Skyrmion spectrum [19, 20]. However, the comparison of the results from $\mathrm{HLS_{SS}}(\pi,\rho)$ and $\mathrm{HLS_{SS}}(\pi,\rho,\omega)$ tells us that, similar to what happens in the Skyrmion case [19, 20], due to the repulsive force arising from the omega meson, the masses of the multi-Skyrmion states are increased.

It is interesting to note that, in contrast to ref. [30], in $\mathrm{HLS_{SS}}(\pi)$ all the states are bound ones owing to the contribution from the higher order terms of HLS. When ρ is included as an explicit degree of freedom in $\mathrm{HLS_{SS}}(\pi,\rho)$ the $B=2$ and 3 states are unbound because their masses are larger than twice and three times of that of the single Skyrmion state, respectively. This is because, when only the π and ρ mesons are included in HLS, the model is very close to the Bogomol'nyi bound, and the force is very weak, as shown in Table 2. This is more evident in the Skyrmion crystal approach to nuclear matter [45] and the $\mathrm{HLS_{BPS}}(\pi,\rho)$ results that will be presented later. However, when the omega meson, the flavor partner of the rho meson, is considered, all the multi-Skyrmion states for $B\geq 2$ are bound, and the binding energies are greater than those in $\mathrm{HLS_{SS}}(\pi,\rho)$. This again shows the significance of the omega force in nuclear physics.

To understand the effects of the hadron resonances, we plotted the contour surfaces of the multi-Skyrmion states with baryon number density $\mathcal{B}^0=0.01$ in Figure 1. Comparing the contours from $\mathrm{HLS_{SS}}(\pi)$ and that from $\mathrm{HLS_{SS}}(\pi,\rho)$, the force from rho meson attracts the constituents of the multi-Skyrmion states closer, although the difference is tiny. However, due to the repulsive force from omega meson, the overlap among the constituents in a multi-Skyrmion state from $\mathrm{HLS_{SS}}(\pi,\rho,\omega)$ is much smaller than others, thereby the omega meson effect is more significant.

Figure 2 depicts the plot of the profile function $F(r)$ in the multi-Skyrmion states. Compared with $\mathrm{HLS_{SS}}(\pi)$, $F(r)$ shrinks in $\mathrm{HLS_{SS}}(\pi,\rho)$ a little bit due to the attraction from the rho meson, as shown in Figure 3 for typical values of B. In contrast to the rho meson, the omega force in $\mathrm{HLS_{SS}}(\pi,\rho,\omega)$ clearly expands the distribution of $F(r)$. The same situation occurs in the profile function $G(r)$ shown in Figure 4. From the expansions of the profile functions, we conclude that the size of the multi-Skyrmion state from $\mathrm{HLS_{SS}}(\pi,\rho,\omega)$ is bigger than the corresponding ones from $\mathrm{HLS_{SS}}(\pi,\rho)$ and $\mathrm{HLS_{SS}}(\pi)$ and the corresponding state from $\mathrm{HLS_{SS}}(\pi,\rho)$ has the smallest size.

3.2.2 *Effect from the warping factor*

Next, we studied the effects of the warping factor by comparing the results calculated from $\mathrm{HLS_{SS}}$ and $\mathrm{HLS_{BPS}}$.

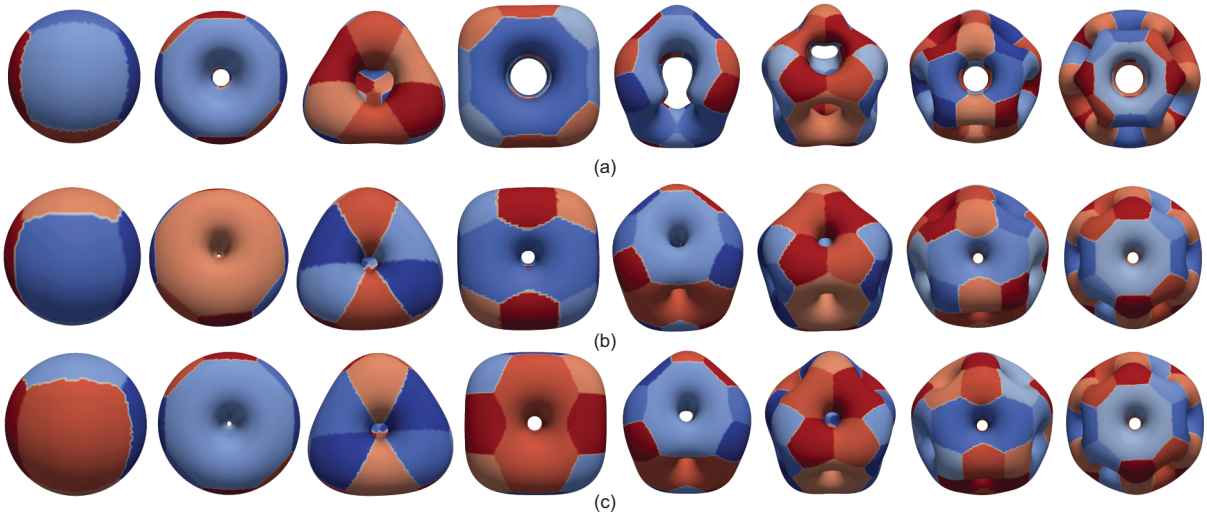

Figure 1 (Color online) Contour surface with $\mathcal{B}^0=0.01$ in the $\mathrm{HLS_{SS}}(\pi,\rho,\omega)$ (a), $\mathrm{HLS_{SS}}(\pi,\rho)$ (b), and $\mathrm{HLS_{SS}}(\pi)$ (c) models for $B=1,2,\cdots,8$ (from left to right).

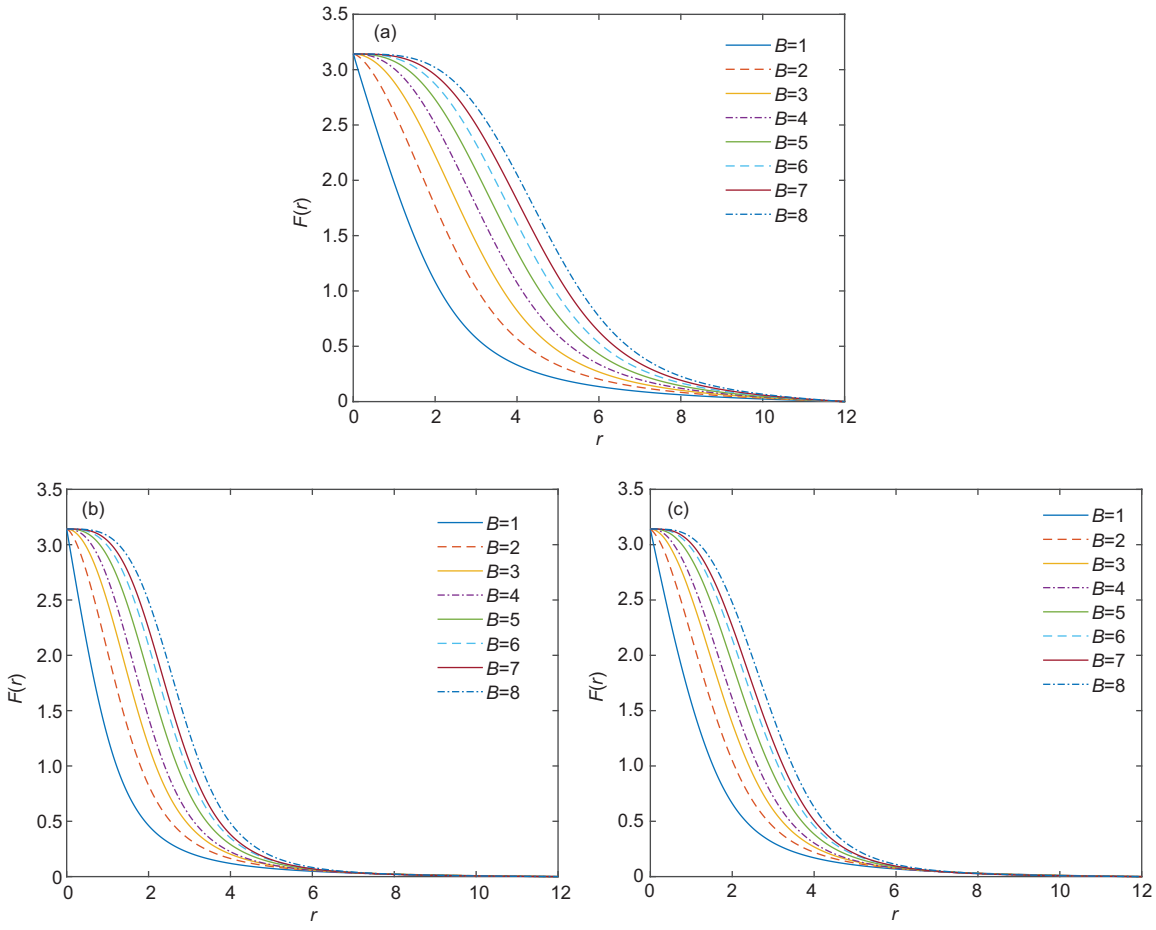

Figure 2 (Color online) Profile function $F(r)$ in $\mathrm{HLS}_{\mathrm{SS}}(\pi,\rho,\omega)$ (a), $\mathrm{HLS}_{\mathrm{SS}}(\pi,\rho)$ (b), and $\mathrm{HLS}_{\mathrm{SS}}(\pi)$ (c) models.

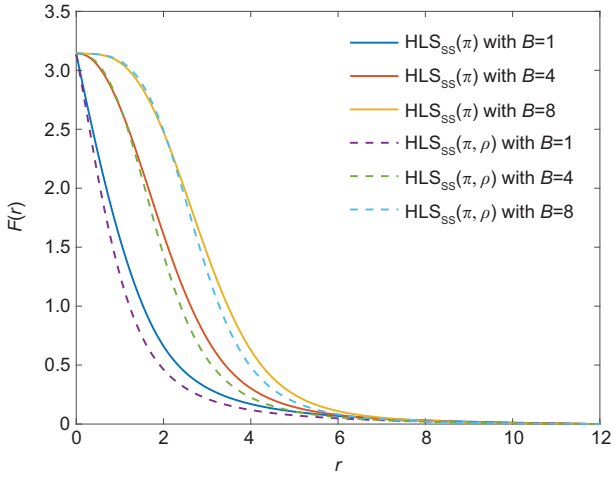

Figure 3 (Color online) Profile function $F(r)$ in $\mathrm{HLS}_{\mathrm{SS}}(\pi,\rho)$ and $\mathrm{HLS}_{\mathrm{SS}}(\pi)$ with $B=1,4,8$.

We first listed the masses of the multi-Skyrmion states in Table 3 for the baryon numbers $B=1,2,\cdots,8$ using the LECs calculated from the BPS model. Similar to the $\mathrm{HLS}_{\mathrm{SS}}$, the results showed that, due to the attractive force from rho meson, the masses of the multi-Skyrmion states from $\mathrm{HLS}_{\mathrm{BPS}}(\pi,\rho)$ are less than those from $\mathrm{HLS}_{\mathrm{BPS}}(\pi)$. However, the repulsive force from omega meson significantly increases the masses. Similar to $\mathrm{HLS}_{\mathrm{SS}}$, all the states in $\mathrm{HLS}_{\mathrm{BPS}}(\pi)$ and $\mathrm{HLS}_{\mathrm{BPS}}(\pi,\rho,\omega)$ are bound ones, whereas all the states from $\mathrm{HLS}_{\mathrm{BPS}}(\pi,\rho)$ listed here are not bound.

Comparing the results from $\mathrm{HLS}_{\mathrm{SS}}$ and $\mathrm{HLS}_{\mathrm{BPS}}$, we showed that due to the warping factor in the SS model, the masses of the multi-Skyrmion states calculated in the former are greater than those in the latter. In the $\mathrm{HLS}_{\mathrm{BPS}}(\pi,\rho)$, the binding energy is very small because the BPS model is close to the BPS limit [43]; thus, it is extremely challenging to form bound states.

Table 4 compares the mass ratio E_B/E_1 of the multi-skyrmions state with baryon number B calculated from different models and empirical values. The results showed that, compared with the truncated BPS(π,ρ) model, the inclusion of the ω meson in $\mathrm{HLS}_{\mathrm{BPS}}$ pushes the ratio closer to the empirical values and, even more, better than that from the truncated BPS(π,ρ,a_1) model. This again indicates the indispensability of the ω meson.

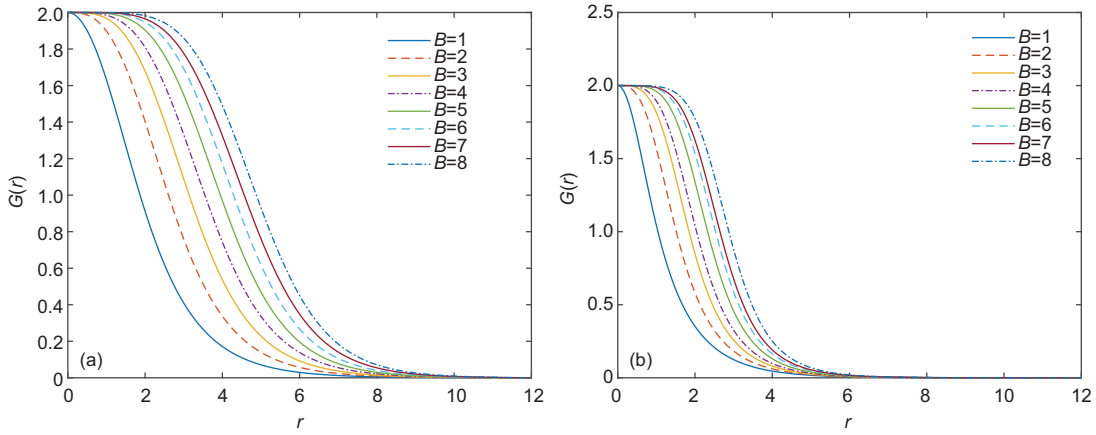

Figure 4 (Color online) Profile function $G(r)$ in $\mathrm{HLS}_{\mathrm{SS}}(\pi,\rho,\omega)$ (a) and $\mathrm{HLS}_{\mathrm{SS}}(\pi,\rho)$ (b) models.

Table 3 Masses of the multi-Skyrmion states in $\mathrm{HLS}_{\mathrm{BPS}}$ (in unit of $4\pi f_\pi^2/m_\rho$). Only the hadron degrees of freedom are explicitly written for simplicity

Model	B							
	1	2	3	4	5	6	7	8
(π,ρ,ω)	8.40	16.74	24.86	32.64	40.73	48.61	56.17	64.25
(π,ρ)	4.17	8.75	13.16	16.93	21.58	25.79	29.25	33.94
(π)	4.87	9.54	14.03	17.94	22.64	26.94	30.59	35.30

Table 4 The ratio of E_B/E_1 in $\mathrm{HLS}_{\mathrm{SS}}(\pi,\rho,\omega)$ and $\mathrm{HLS}_{\mathrm{BPS}}(\pi,\rho,\omega)$. The results from the truncated BPS [27] and experimental data are included for comparison

Model	B			
	1	2	3	4
$\mathrm{HLS}_{\mathrm{SS}}(\pi,\rho,\omega)$	1	1.967	2.903	3.776
$\mathrm{HLS}_{\mathrm{BPS}}(\pi,\rho,\omega)$	1	1.993	2.960	3.886
Truncated BPS(π,ρ)	1	1.961	2.908	3.843
Truncated BPS(π,ρ,a_1)	1	1.968	2.926	3.886
Experimental data	1	1.998	2.991	3.969

To further understand the effect of the warping factor, we compared the contour surface of the baryon number density. Here, we considered the results from $\mathrm{HLS}_{\mathrm{SS}}(\pi,\rho)$ and $\mathrm{HLS}_{\mathrm{BPS}}(\pi,\rho)$ as examples and plotted the results for the baryon number density $\mathcal{B}^0 = 0.01$ in Figure 5. This figure explicitly shows that the constituents of the multi-Skyrmion states are far away from each other due to the warping factor in the SS model. Since the constituents are further, the distributions of the profile functions are more expanded in $\mathrm{HLS}_{\mathrm{SS}}$ as shown in Figure 6.

4 Summary and discussion

Using the HLS approach, we introduced the vector mesons ρ and ω into the Skyrme model and calculated the effect of vector mesons on the multi-Skyrmion states with baryon numbers from $B = 1$ to 8. With the help of the holographic models, all the LECs can be self-consistently calculated using two inputs f_π and m_ρ. In this sense, we explicitly studied the effects of the vector mesons and the warping factor on the properties of multi-Skyrmion states.

The main conclusions of this work can be summarized as follows: compared with the model with only pion, the ρ meson slightly reduces the mass of the multi-Skyrmion states as well as the size of the profile function $F(r)$. The effect of the ω meson on multi-Skyrmion states is obvious, not only on increases in the masses of the multi-Skyrmion states but also on expansions of the sizes of the states. The contribution from the warping factor cannot be ignored when estimating the LECs of the HLS using the holographic models of QCD.

Given the above qualitative conclusions, several extensions of this work can be expected.

In this research, we calculated the LECs using the SS and the BPS models. It is well known that the hadron spectrum, including that of the skyrmions, does not agree with the empirical values. In avoiding this defect, it is interesting to resort to certain holographic models that yield hadron properties consistent with nature. A possible approach is to use the holographic model from the bottom-up approach, for example, the soft-wall model developed in refs. [46, 47], using the approach developed in ref. [48]. Furthermore, in this approach, the explicit chiral symmetry-breaking effect, which is ignored in this research but is found significant for the spectrum and shapes of the multi-Skyrmion states, can be self-consistently considered.

A generic problem in the Skyrmion approach to nuclear physics is that both the masses of the baryons and binding energies between skyrmions are too large to confront the empirical values. Some modified Skyrme models, such as the BPS Skyrme model [49] and the false vacuum model [50], showed promise for overcoming these issues. Consequently, it is interesting to examine the properties of the multi-Skyrmion

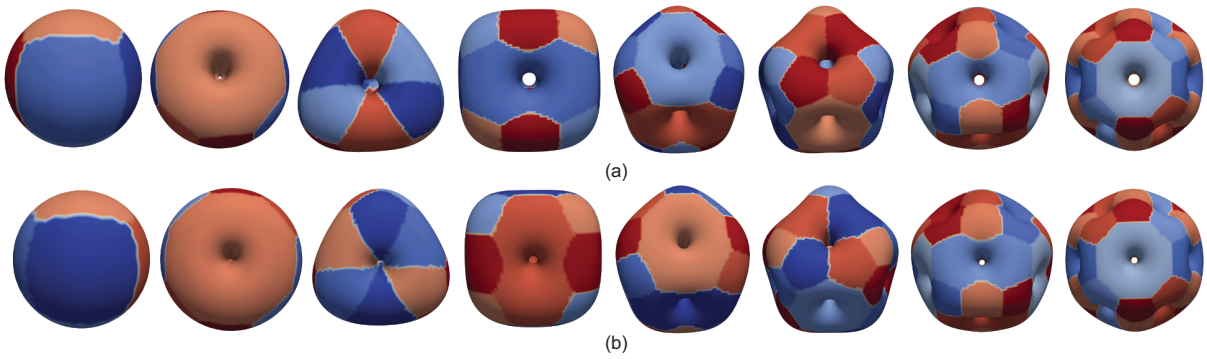

Figure 5 (Color online) Contour surface with $\mathcal{B}^0 = 0.01$ in the $\mathrm{HLS}_{\mathrm{SS}}(\pi,\rho)$ model (a) and $\mathrm{HLS}_{\mathrm{BPS}}(\pi,\rho)$ model (b) for $B = 1, 2, \cdots, 8$ (from left to right).

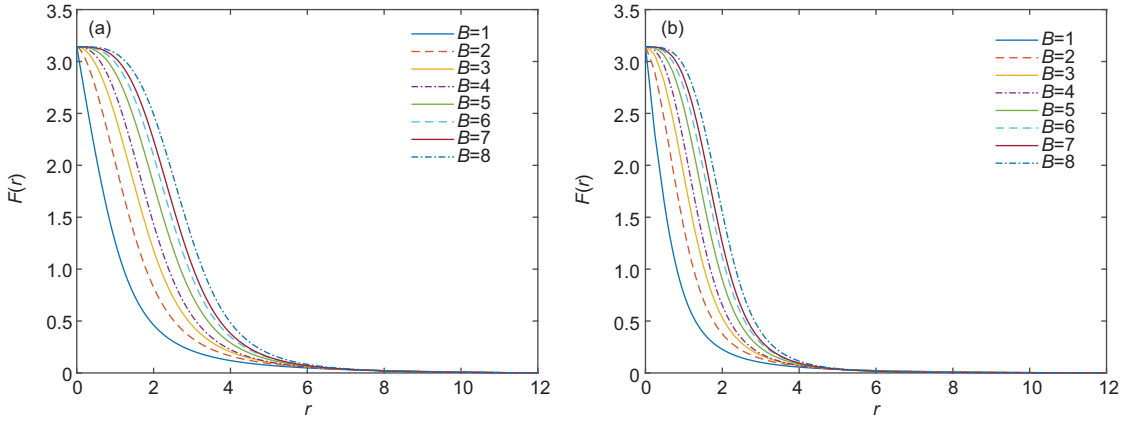

Figure 6 (Color online) Profile functions $F(r)$ in $\mathrm{HLS}_{\mathrm{SS}}(\pi,\rho)$ model (a) and $\mathrm{HLS}_{\mathrm{BPS}}(\pi,\rho)$ model (b).

states using these models.

In general, the isospin unit vector $\hat{\boldsymbol{n}}$ in the parametrization of the rho meson (17) should differ from that in the parametrization of the pion field (16). Conversely, there should be two different vectors, $\hat{\boldsymbol{n}}^{\rho}$ for the rho field and $\hat{\boldsymbol{n}}^{\pi}$ for the pion field; since they are independent fields, similar to the Skyrmion crystal approach to nuclear matter [51, 52]. We checked such a senario that $\hat{\boldsymbol{n}}^{\pi}$ and $\hat{\boldsymbol{n}}^{\rho}$ are differently parameterized. The minimal mass of the multi-Skyrmion state can only be obtained using the same form of parameterization previously used.

To see the effects of the vector mesons and warping factor, we focused on the rational map ansatz here, which works well in the absence of pion mass [30, 39]—a situation also considered in this research. The rational map ansatz does not always yield the global minima for some specific models and multi-Skyrmion states. For example, the instanton approximation [26] and the ADHM skyrmions [53, 54] could reduce the binding energy about 2%. When a big pion mass is considered, soliton solutions with lower symmetry play an important role in the cluster structure of the nucleus; however, these solutions cannot be described by rational map simplely [34, 55], but a product ansatz is preferred. Thus, the rational map ansatz and other approaches should be equally checked to confirm the real structure of the multi-Skyrmion states.

Yong-Liang Ma was supported by the National Natural Science Foundation of China (Grant Nos. 11875147, and 12147103). We would like to thank Yu Tian and Hong-Bao Zhang for their valuable discussions.

Conflict of interest The authors declare that they have no conflict of interest.

1 T. H. R. Skyrme, Proc. Roy. Soc. Lond. A **260**, 127 (1961).
2 T. H. R. Skyrme, Nucl. Phys. **31**, 556 (1962).
3 M. Rho, and I. Zahed, *The Multifaceted Skyrmions*, 2nd ed. (World Scientific, Singapore, 2016).
4 I. Zahed, and G. E. Brown, Phys. Rep. **142**, 1 (1986).
5 Y. L. Ma, and M. Rho, Sci. China-Phys. Mech. Astron. **60**, 032001 (2017).
6 Y. L. Ma, and M. Rho, Prog. Particle Nucl. Phys. **113**, 103791 (2020).
7 N. S. Manton, *Skyrmions: A Theory of Nuclei* (World Scientific, Singapore, 2022).
8 E. Witten, Nucl. Phys. B **160**, 57 (1979).
9 E. Witten, Nucl. Phys. B **223**, 433 (1983).
10 E. Witten, Nucl. Phys. B **223**, 422 (1983).
11 I. Zahed, U. G. Meissner, and U. B. Kaulfuss, Nucl. Phys. A **426**, 525

(1984).
12 U. G. Meissner, N. Kaiser, A. Wirzba, and W. Weise, Phys. Rev. Lett. **57**, 1676 (1986).
13 Y. Igarashi, M. Hohmura, A. Kobayashi, H. Otsu, T. Sato, and S. Sawada, Nucl. Phys. B **259**, 721 (1985).
14 A. Drago, and V. Mantovani Sarti, Phys. Rev. C **86**, 015211 (2012).
15 M. Abu-Shady, and M. Rashdan, Phys. Rev. C **81**, 015203 (2010).
16 D. Parganlija, F. Giacosa, and D. H. Rischke, Phys. Rev. D **82**, 054024 (2010).
17 U. G. Meissner, Phys. Rep. **161**, 213 (1988).
18 K. Nawa, H. Suganuma, and T. Kojo, Phys. Rev. D **75**, 086003 (2007).
19 Y. L. Ma, Y. Oh, G. S. Yang, M. Harada, H. K. Lee, B. Y. Park, and M. Rho, Phys. Rev. D **86**, 074025 (2012).
20 Y. L. Ma, G. S. Yang, Y. Oh, and M. Harada, Phys. Rev. D **87**, 034023 (2013).
21 T. Sakai, and S. Sugimoto, Prog. Theor. Phys. **113**, 843 (2005).
22 T. Sakai, and S. Sugimoto, Prog. Theor. Phys. **114**, 1083 (2005).
23 M. Bando, T. Kugo, S. Uehara, K. Yamawaki, and T. Yanagida, Phys. Rev. Lett. **54**, 1215 (1985).
24 M. Bando, T. Kugo, and K. Yamawaki, Phys. Rep. **164**, 217 (1988).
25 M. Harada, and K. Yamawaki, Phys. Rep. **381**, 1 (2003).
26 P. Sutcliffe, J. High Energ. Phys. **2010(8)**, 019 (2010).
27 P. Sutcliffe, J. High Energ. Phys. **2011(4)**, 045 (2011).
28 R. A. Battye, and P. M. Sutcliffe, Phys. Lett. B **391**, 150 (1997).
29 S. B. Gudnason, and C. Halcrow, Phys. Rev. D **97**, 125004 (2018).
30 C. J. Houghton, N. S. Manton, and P. M. Sutcliffe, Nucl. Phys. B **510**, 507 (1998).
31 S. Krusch, Ann. Phys. **304**, 103 (2003).
32 S. B. Gudnason, Phys. Rev. D **98**, 096018 (2018).
33 H. Weigel, B. Schwesinger, and G. Holzwarth, Phys. Lett. B **168**, 321 (1986).
34 R. Battye, N. S. Manton, and P. Sutcliffe, Proc. Roy. Soc. Lond. A **463**, 261 (2007).
35 S. Nelmes, and B. M. A. G. Piette, Phys. Rev. D **84**, 085017 (2011).
36 B. Y. Park, W. G. Paeng, and V. Vento, Nucl. Phys. A **989**, 231 (2019).
37 R. A. Battye, and P. M. Sutcliffe, Phys. Rev. Lett. **79**, 363 (1997).
38 R. A. Battye, and P. M. Sutcliffe, Nucl. Phys. B **705**, 384 (2005).
39 C. Naya, and P. Sutcliffe, J. High Energ. Phys. **2018(05)**, 174 (2018).
40 C. Naya, and P. Sutcliffe, Phys. Rev. Lett. **121**, 232002 (2018).
41 U. G. Meissner, N. Kaiser, and W. Weise, Nucl. Phys. A **466**, 685 (1987).
42 H. Imai, A. Kobayashi, H. Otsu, and S. Sawada, Prog. Theor. Phys. **82**, 141 (1989).
43 P. Sutcliffe, Phys. Rev. D **79**, 085014 (2009).
44 E. Bueler, *PETSc for Partial Differential Equations: Numerical Solutions in C and Python* (Society for Industrial and Applied Mathematics, Philadelphia, 2020).
45 Y. L. Ma, M. Harada, H. K. Lee, Y. Oh, B. Y. Park, and M. Rho, Phys. Rev. D **88**, 014016 (2013) [Erratum: Phys. Rev. D **88**, 079904 (2013)].
46 L. X. Cui, Z. Fang, and Y. L. Wu, Eur. Phys. J. C **76**, 22 (2016).
47 Z. Fang, Y. L. Wu, and L. Zhang, Phys. Rev. D **100**, 054008 (2019).
48 M. Harada, Y. L. Ma, and S. Matsuzaki, Phys. Rev. D **89**, 115012 (2014).
49 C. Adam, C. Naya, J. Sanchez-Guillen, and A. Wereszczynski, Phys. Rev. Lett. **111**, 232501 (2013).
50 L. A. Ferreira, and L. R. Livramento, J. Phys. G-Nucl. Part. Phys. **49**, 115102 (2022).
51 B. Y. Park, M. Rho, and V. Vento, Nucl. Phys. A **736**, 129 (2004).
52 G. Barriga, F. Canfora, M. Lagos, M. Torres, and A. Vera, Nucl. Phys. B **983**, 115913 (2022).
53 J. Cork, and C. Halcrow, Nonlinearity **35**, 3944 (2022).
54 M. F. Atiyah, N. J. Hitchin, V. G. Drinfeld, and Y. I. Manin, Phys. Lett. A **65**, 185 (1978).
55 R. A. Battye, and P. M. Sutcliffe, Phys. Rev. C **73**, 055205 (2006).

Appendix Mass of the multi-Skyrmion state in the hidden local symmetry

In this appendix, we provide the expression of the mass of the multi-Skyrmion state using the Lagrangian (7). In accordance with this Lagrangian, we decompose the mass as:

$$M = M_{(2)} + \sum_{i=1}^{9} y_i \frac{1}{2} a g^2 M_{y_i} + z_4 a g^2 m_{z_4} + z_5 a g^2 M_{z_5} + \sum_{i=1}^{3} c_i \frac{a g^3 N_c}{16\pi^2} M_{c_i}. \tag{1}$$

In unit of the scale factor $4\pi\frac{f_\pi^2}{m_\rho}$, we explicitly have

$$M_{(2)} = \int \mathrm{d}r \left\{ \frac{1}{2} r^2 F'^2 + n \sin^2 F - \frac{a g^2}{2} r^2 W^2 - \frac{a g^2}{2} r^2 W'^2 + an(G-1+\cos F)^2 + anG'^2 + \frac{aI}{2r^2} G^2 (G-2)^2 \right\},$$

$$M_{y_1} = -\int \mathrm{d}r \left(\frac{1}{4} r^2 F'^4 + nF'^2 \sin^2 F + \frac{I}{r^2} \sin^4 F \right),$$

$$M_{y_2} = -\int \mathrm{d}r \left(\frac{1}{4} r^2 F'^4 - nF'^2 \sin^2 F \right),$$

$$M_{y_3} = \int \mathrm{d}r \left(-\frac{g^4}{4} r^2 W^4 + g^2 W^2 n (G-1+\cos F)^2 - \frac{I}{r^2} (G-1+\cos F)^4 \right),$$

$$M_{y_4} = \int \mathrm{d}r \left(-\frac{g^4}{4} r^2 W^4 + g^2 W^2 n (G-1+\cos F)^2 \right),$$

$$M_{y_5} = \int \mathrm{d}r \left(\frac{g^2}{4} r^2 W^2 F'^2 - \frac{1}{2} nF'^2 (G-1+\cos F)^2 + \frac{1}{2} g^2 n W^2 \sin^2 F - \frac{I}{r^2} \sin^2 F (G-1+\cos F)^2 \right),$$

$$M_{y_6} = 0,$$

$$M_{y_7} = -\int \mathrm{d}r \frac{I}{r^2} \sin^2 F (G-1+\cos F)^2,$$

$$
\begin{aligned}
M_{y_8} =& 2\int \mathrm{d}r\frac{I}{r^2}\sin^2 F(G-1+\cos F)^2,\\
M_{y_9} =& \frac{1}{2}\int \mathrm{d}r\left(\frac{1}{2}g^2W^2F'^2r^2+g^2W^2n\sin^2 F+F'^2n(G-1+\cos F)^2\right),\\
M_{z_4} =& \int \mathrm{d}r\left(-nF'G'\sin F+\frac{I}{2r^2}\sin^2 FG(G-2)\right),\\
M_{z_5} =& \int \mathrm{d}r\frac{I}{2r^2}(G-1+\cos F)^2G(G-2),\\
M_{c_1} =& \int \mathrm{d}r\left(nWF'(G-1+\cos F)^2+3nWF'\sin^2 F\right),\\
M_{c_2} =& \int \mathrm{d}r\left(nWF'(G-1+\cos F)^2-3nWF'\sin^2 F\right),\\
M_{c_3} =& 2\int \mathrm{d}r\left(nW\sin FG'-nW'\sin F(G-1+\cos F)-\frac{1}{2}nWF'G(G-2)\right),
\end{aligned}
\tag{a2}
$$

where baryon number n and function I are defined as:

$$
n=\frac{1}{4\pi}\int\left(\frac{1+|z|^2}{1+|R|^2}\left|\frac{\mathrm{d}R}{\mathrm{d}z}\right|\right)^2\frac{2\mathrm{i}\mathrm{d}z\mathrm{d}\bar{z}}{(1+|z|^2)^2},
\tag{a3}
$$

and

$$
I=\frac{1}{4\pi}\int\left(\frac{1+|z|^2}{1+|R|^2}\left|\frac{\mathrm{d}R}{\mathrm{d}z}\right|\right)^4\frac{2\mathrm{i}\mathrm{d}z\mathrm{d}\bar{z}}{(1+|z|^2)^2}.
\tag{a4}
$$